J Mater Sci (2010) 45:2030–2034
DOI 10.1007/s10853-009-3713-3

HTC2009

Liquid–liquid phase equilibria, density difference, and interfacial tension in the Al–Bi–Si monotectic system

I. Kaban · J. Gröbner · W. Hoyer · R. Schmid-Fetzer

Received: 12 May 2009 / Accepted: 27 June 2009 / Published online: 8 July 2009

Abstract We have performed thermodynamic calculation of the phase equilibria in the ternary monotectic system Al–Bi–Si. The liquid–liquid miscibility gap in the Al–Bi–Si system extends over almost the entire concentration triangle. The thermal analysis data for $(Al_{0.345}Bi_{0.655})_{100-x}Si_x$ alloys ($x = 2.5$, 5, 7.5, and 10 wt%) excellently agree with the calculated phase diagram. The experimental density difference of the coexisting liquid phases shows a good agreement with the density difference calculated in the approximation of ideal solution using the densities of pure elements and the compositions of L′ and L″ from the thermodynamic calculation. The liquid–liquid interfacial tension in the $(Al_{0.345}Bi_{0.655})_{100-x}Si_x$ liquid alloys increases with Si content. The experimental temperature dependence of the interfacial tension is well described by the power low in reduced temperature (T_C–T) at approach of the critical temperature with the exponent $\mu = 1.3$, which is close to the value predicted by the renormalization group theory of critical behavior.

Introduction

Multicomponent alloys showing liquid–liquid immiscibility within a certain composition and temperature range (monotectic alloys) solidify at normal conditions into layered structures, and this is their main shortcoming in a view of practical application [1]. The experimental investigations and modeling of the microstructure development during cooling of the monotectic alloys are carried out in order to learn how the phase separation can be suppressed or controlled at least. The liquid–liquid (l–l) interfacial energy and density difference play a crucial role in the demixing process. Therefore, the composition of coexisting phases, density, and the interfacial tension between the two liquid phases in dependence on the temperature should be known [1–3].

In this study, we present the results of the thermodynamic calculation of the phase equilibria in the Al–Bi–Si system and the experimental investigation of the liquid–liquid density difference and interfacial tension in the ternary alloys $(Al_{0.345}Bi_{0.655})_{100-x}Si_x$ ($x = 2.5, 5, 7.5$, and 10 wt%).

Al–Bi–Si phase equilibria

Earlier, phase equilibria in the ternary system Al–Bi–Si were thermodynamically optimized by Yu [4] using the software developed by Lukas et al. [5]. In the present study, we calculate the phase equilibria in the Al–Bi–Si system using the CALPHAD approach and PANDAT software as described elsewhere [6]. For the unary phases, the Gibbs energy functions are taken from the SGTE compilation by Dinsdale [7]. The parameters for binary Al–Bi system are from our recent optimization [8], and those for Al–Si and Bi–Si were taken from the works of Gröbner et al. [9] and Olesinski and Abbaschian [10], respectively. Ternary parameters were not used for this calculation. All parameters are listed in Table 1.

The calculated liquidus projection is shown in Fig. 1, while the calculated phase diagram vertical section along the sample compositions studied in this work is plotted in Fig. 2. The monotectic Al–Bi–Si system is characterized

I. Kaban (✉) · W. Hoyer
Institute of Physics, Chemnitz University of Technology, 09107 Chemnitz, Germany
e-mail: ivan.kaban@physik.tu-chemnitz.de

J. Gröbner · R. Schmid-Fetzer
Institute of Metallurgy, Clausthal University of Technology, Robert-Koch-Str. 42, 38678 Clausthal-Zellerfeld, Germany

Table 1 Thermodynamic parameters for the Al–Bi–Si system

System	Phase	Parameters (J/mol-atoms)	References
Al–Bi	Liquid	$L^{0,\text{Liquid}}_{\text{Al,Bi}} = +23300 - 1.665989 \cdot T$	[8]
		$L^{1,\text{Liquid}}_{\text{Al,Bi}} = +13668.3 - 6.547643 \cdot T$	
		$L^{2,\text{Liquid}}_{\text{Al,Bi}} = +19682.3 - 13.657834 \cdot T$	
		$L^{3,\text{Liquid}}_{\text{Al,Bi}} = +6573.75 - 1.8075 \cdot T$	
Bi–Si	Liquid	$L^{0,\text{Liquid}}_{\text{Bi,Si}} = +46370 + 2.26 \cdot T$	[10]
Al–Si	Liquid	$L^{0,\text{Liquid}}_{\text{Al,Si}} = -11340.1 - 1.23394 \cdot T$	[9]
		$L^{1,\text{Liquid}}_{\text{Al,Si}} = -3530.93 + 1.35993 \cdot T$	
		$L^{2,\text{Liquid}}_{\text{Al,Si}} = +2265.39$	
	(Al) FCC	$L^{0,\text{FCC}}_{\text{Al,Si}} = -3143.78 + 0.39297 \cdot T$	[9]
	(Si) diamond	$L^{0,\text{diamond}}_{\text{Al,Si}} = +113346 - 47.5551 \cdot T$	[9]

Unary functions for the elements are taken from Dinsdale [7]

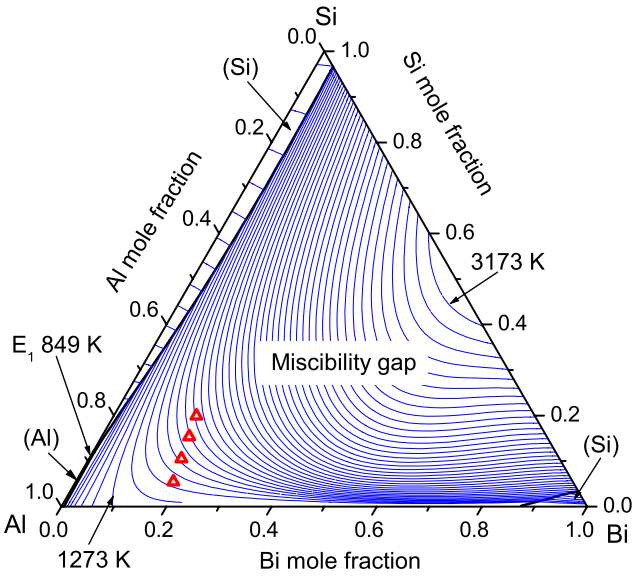

Fig. 1 Calculated liquidus projection of the Al–Bi–Si system (in at.%): *thick lines* (*black*)—the liquidus edges; *thin lines* (*blue*)—the isothermal lines. The isothermal lines are shown with the interval of 50 K. Two isothermal lines (1273 and 3173 K) are marked

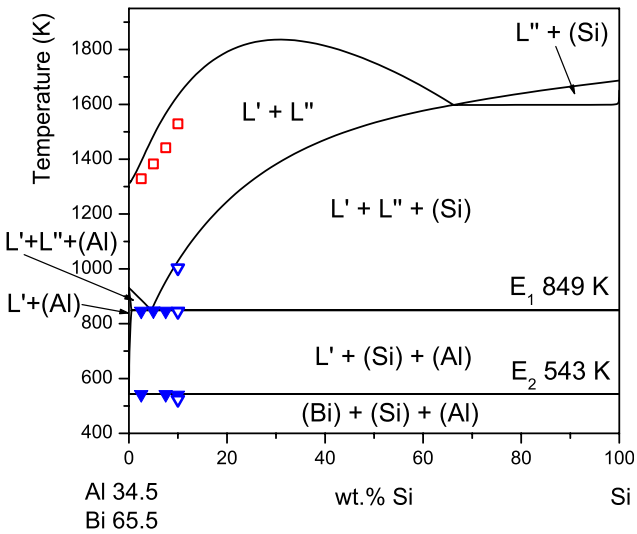

Fig. 2 Calculated vertical phase diagram through the $(Al_{0.345}Bi_{0.655})_{100-x}Si_x$ section (wt%) and experimental data: *solid triangles*—extracted from thermal analysis in this study; *open triangles*—from the DSC measurement [15]; *open squares*—critical temperatures from Table 2

by the large miscibility gap covering almost the entire concentration triangle.

Experimental details

$(Al_{0.345}Bi_{0.655})_{100-x}Si_x$ alloys ($x = 2.5$, 5, 7.5, and 10 wt%) were prepared from high-purity Al, Bi, and Si (99.999%). The position of these alloys on the Al–Bi–Si concentration triangle is shown in Fig. 1. The compositions in at.% are given in Table 2. Because of a high melting temperature of Si, the proper quantities of Al and Si were firstly melted together by arc-melting in an atmosphere of Ar. The Al–Si ingots and Bi pieces in proper quantities were used for the investigations.

Liquid–liquid interfacial tension $\sigma_{L'L''}$ and difference in macroscopic densities of two coexisting liquid phases $\Delta\rho_{L'L''}$ have been measured by a tensiometric technique described in detail elsewhere [8, 11–15]. Relative error of the density difference is estimated to be 3%. The error of interfacial tension is about 5% near the monotectic temperature. As in conventional thermal analysis, temperature–time curves were taken for the samples during free cooling. The temperature was measured with accuracy better than ± 3 K by the thermocouple inserted into a bore in the bottom of the sample crucible.

Results and discussion

Figure 2 demonstrates an excellent agreement of the calculated vertical phase diagram through the $(Al_{0.345}Bi_{0.655})_{100-x}Si_x$ section (wt%) with the present thermal analysis results. Also, a good agreement with the DSC data

Table 2 Temperature dependence of the liquid–liquid interfacial tension $\sigma_{L'L''}$: the fits to the experimental data

Alloy composition		Fit $\sigma_{L'L''} = \sigma_0 \cdot (1-T/T_C)^{\mu}$ (mN/m)		
Weight percent	Atomic percent	Fitting range (K)	T_C (K)	σ_0 (mN/m)
$Al_{34.5}Bi_{65.5}$	$Al_{80.31}Bi_{19.69}$	933–1213	1310	291
$(Al_{0.345}Bi_{0.655})_{97.5}Si_{2.5}$	$Al_{75.96}Bi_{18.62}Si_{5.42}$	893–1193	1329	273
$(Al_{0.345}Bi_{0.655})_{95}Si_5$	$Al_{71.86}Bi_{17.61}Si_{10.53}$	873–1238	1383	263
$(Al_{0.345}Bi_{0.655})_{92.5}Si_{7.5}$	$Al_{67.99}Bi_{16.66}Si_{15.35}$	943–1193	1442	258
$(Al_{0.345}Bi_{0.655})_{90}Si_{10}$	$Al_{64.33}Bi_{15.77}Si_{19.9}$	1023–1193	1529	227

σ_0 is a constant, T is the absolute temperature, and T_C is the critical temperature. The critical exponent $\mu = 1.3$ was fixed during the fitting

for the $(Al_{0.345}Bi_{0.655})_{90}Si_{10}$ composition from [15] is observed. Somewhat lower temperature values in the DSC experiment are explained by the high cooling rate (20 K/min). Unfortunately, due to very high critical temperature T_C, as it follows from the thermodynamic calculations, and high vapor pressure of Bi, we could not determine T_C experimentally.

Experimental temperature dependences of the density difference of coexisting liquid phases $\Delta\rho_{L'L''}$ in the Al–Bi–Si alloys are plotted in Fig. 3. It would be better to analyze molar volumes of the coexisting phases $V_{L'}$ and $V_{L''}$ or their difference $\Delta V_{L'L''}$ rather than the density difference. In the approximation of ideal solution, the molar volumes $V_{L'}$ and $V_{L''}$ can easily be calculated from the linear molar composition variation, which follows from known compositions of L′ and L″ in the phase diagram and the molar volumes (or densities) of pure liquid components. However, it is not possible to find the difference of molar volumes of L′ and L″ from their density difference, which is the only quantity measured experimentally. Therefore, using the composition data of the present thermodynamic model, we have calculated the densities of Al-rich liquid $\rho_{L'}$ and Bi-rich liquid $\rho_{L''}$ assuming an ideal solution, and defined this as the theoretical density difference $\Delta\rho_{L'L''}$. The densities of the pure elements were taken from Iida and Guthrie [16]. The good agreement observed over the entire experimentally accessible temperature range between the measured and theoretically calculated density difference suggests reliability of the data for the compositions of coexisting liquids obtained by the thermodynamic calculation in this study.

Figure 4 shows the experimental values of the (l–l) interfacial tension $\sigma_{L'L''}$ in the ternary monotectic alloys $(Al_{0.345}Bi_{0.655})_{100-x}Si_x$ in comparison with the (l–l) interfacial tension for the liquid $Al_{34.5}Bi_{65.5}$ (wt%) [13]. The interfacial tension between Al-rich and Bi-rich liquid phases as well as the critical temperature T_C increases upon addition of Si. This finding agrees with the thermodynamics of the Al–Bi–Si system expressed in the calculated phase diagram (Fig. 1). Interfacial tension is a functional of the concentration profile at the liquid–liquid interface and can be expressed by the Eq. 1 obtained by Hoyt [17], who

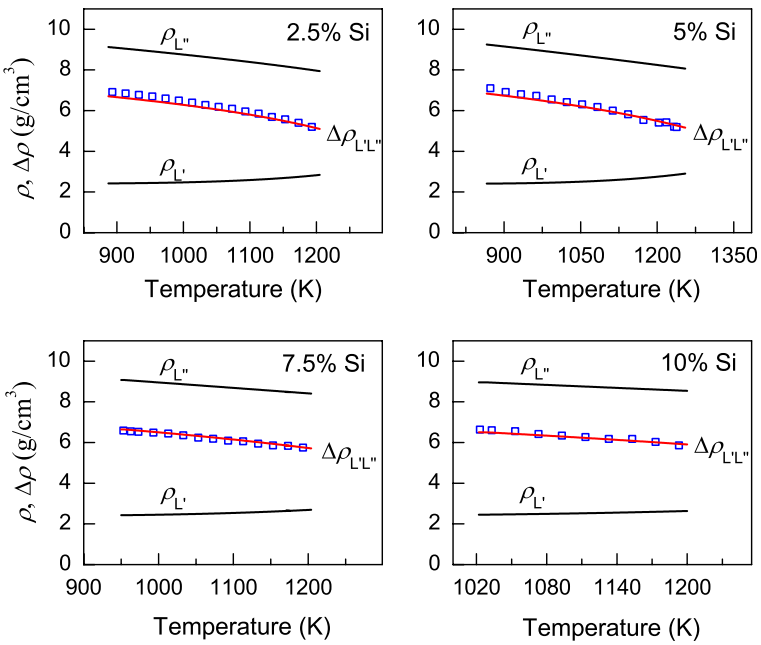

Fig. 3 Theoretical and experimental temperature dependence of the densities of Al-rich liquid $\rho_{L'}$ and Bi-rich liquid $\rho_{L''}$ and the density difference $\Delta\rho_{L'L''}$ for liquid $(Al_{0.345}Bi_{0.655})_{100-x}Si_x$ alloys (wt%): *symbols*—experimental values; *lines*—calculated in the approximation of ideal solution with the densities of pure elements [16] and compositions of liquid phases determined in this study. Experimental error is comparable with the size of symbols

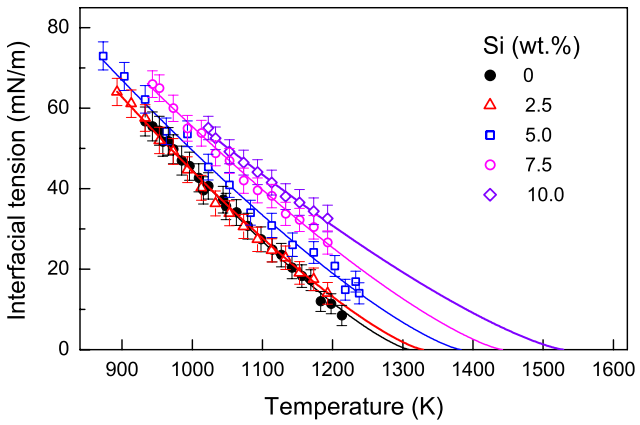

Fig. 4 Temperature dependence of the interfacial tension in $(Al_{0.345}Bi_{0.655})_{100-x}Si_x$ alloys (wt%)

extended the Cahn-Hilliard theory [18] to multicomponent systems:

$$\sigma_{L/L''} = N_V \int_{-\infty}^{+\infty} \left[\Delta f(c_1, c_2, .., c_{n-1}) + \sum_i^{n-1} \sum_j^{n-1} \kappa_{ij} \nabla c_i \nabla c_j \right] dx. \quad (1)$$

Here, N_V is the number of molecules per unit volume, c_i is the mole fraction of component i, n is the number of components, κ_{ij} is the energy coefficient associated with the composition gradients $\nabla c_i \nabla c_j$. $\Delta f(c_i)$ is a free energy referred to a standard state of an equilibrium mixture. The composition variation across the interface, which determines the contribution of the gradient energy term to the interfacial tension, depends on the composition of bulk phases and the size of the miscibility gap. Therefore, it is reasonable to expect an increase of the concentration gradient with widening miscibility gap. This, in due course, suggests an increase of the interfacial tension if the miscibility gap extends, what is observed in the Al–Bi–Si monotectic system indeed.

It has been shown earlier [13–15] that the experimental temperature dependence of the (l–l) interfacial tension for Al-based monotectic alloys is well described by the power law

$$\sigma_{L/L''} = \sigma_0 \cdot (1 - T/T_C)^{\mu} \quad (2)$$

where σ_0 is a constant, T is the absolute temperature, T_C is the critical temperature, and μ is the so-called critical-point exponent. For the $Al_{34.5}Bi_{65.5}$ binary and $(Al_{0.345}Bi_{0.655})_{90}Sn_{10}$ ternary alloys, where the interfacial tension was measured practically over the whole miscibility gap temperature region, $\mu \approx 1.3$ was obtained [13, 15]. This value is close to the prediction of the renormalization group theory of critical behavior [19], which gives $\mu = 1.26$. In the present study, we have fitted the experimental interfacial tension for $(Al_{0.345}Bi_{0.655})_{100-x}Si_x$ alloys with the Eq. 2 leaving σ_0 and T_C parameters free, while μ was fixed (both values, 1.26 and 1.3 were tested). In the fitting range, difference between the fitting functions with $\mu = 1.3$ and $\mu = 1.26$ is not significant (less than 1.5%). The critical temperatures determined by the $\sigma_{\alpha\beta}(T)$ fitting with $\mu = 1.26$ were about 9 K lower as compared to the fits with $\mu = 1.3$. The fitting curves obtained with $\mu = 1.3$ are shown in Fig. 4 and their parameters are listed in Table 2.

It has to be noted that the error in T_C determined by the $\sigma_{\alpha\beta}(T)$ fitting can be high for large Si concentrations because the experimental data cover only about half the miscibility gap height. This might explain why the critical temperatures for $(Al_{0.345}Bi_{0.655})_{100-x}Si_x$ alloys determined from the experimental temperature dependences of the interfacial tension fall into the calculated miscibility gap as it shown by *open squares* in Fig. 2. Also, it should be taken into account that thermodynamic calculation provides only an upper limit on the critical temperature because it uses a classical model for the Gibbs energy, which gives the exponent of $\frac{1}{2}$ for the difference in composition of the coexisting liquid phases on approach to T_C, while the exponent determined from experiments is about $\frac{1}{3}$ [19–21]. The critical temperature in the Bi–Si binary calculated with the parameters of Olesinski and Abbaschian [10], which are used by us, is about 1390 K above the boiling point of pure Bi and, thus, cannot be proven experimentally. This all might result in the overestimation of the height of the liquid–liquid miscibility gap in Al–Bi–Si system in our calculation.

Conclusions

We have calculated the phase equilibria in the ternary monotectic system Al–Bi–Si using the thermodynamic data for unary phases and respective three binary systems. The liquid–liquid miscibility gap in the Al–Bi–Si system extends over almost the entire concentration triangle. The experimental data for $(Al_{0.345}Bi_{0.655})_{100-x}Si_x$ alloys (x = 2.5, 5, 7.5, and 10 wt%) extracted from the thermal analysis excellently agree with the calculated phase diagram. Also, the density difference of the coexisting liquid phases exhibits a good agreement with the density difference calculated in the approximation of ideal solutions using the densities of pure elements and the compositions of L′ and L″ from the thermodynamic calculations.

The increase of the interfacial tension in the $(Al_{0.345}Bi_{0.655}S)_{100-x}Si_x$ liquid alloys upon increasing Si content correlates with the widening of the liquid–liquid miscibility gap. The temperature dependence of the interfacial tension can be well described by the power law $\sigma_{L'L''} = \sigma_0 \cdot (1–T/T_C)^{\mu}$ with the exponent $\mu = 1.3$, which is close to

the value predicted by the renormalization group theory of critical behavior ($\mu = 1.26$).

Out study demonstrates that experimental data on the interfacial tension and difference in densities of coexisting liquid phases in monotectic systems may provide information on the bulk phase diagram and critical temperature, which can hardly be obtained by other methods.

Acknowledgements This study was financially supported by the German Research Foundation (DFG).

References

1. Ratke L, Diefenbach S (1995) Mat Sci Eng R15:263
2. Ratke L, Drees S, Diefenbach S, Prinz B, Ahlborn H (1996) In: Ratke L (ed) Materials and fluids under low gravity. Springer, Berlin
3. Tang H, Wrobel LC, Fan Z (2005) Appl Phys A 81:549
4. Yu S-K (1994) Ph.D. Thesis, Stuttgart University
5. Lukas HL, Fries S, Kattner U, Weiss J (1991) Manual of the computer programs BINGSS, BINFKT, TERGSS and TERFKT, Version 91-3
6. Schmid-Fetzer R, Gröbner J (2001) Adv Eng Mater 3:947
7. Dinsdale AT (1991) Calphad 15:317
8. Mirković D, Gröbner J, Kaban I, Hoyer W, Schmid-Fetzer R (2009) Int J Mater Res (Z Metallkd) 100:176
9. Gröbner J, Lukas HL, Aldinger F (1996) Calphad 20:247
10. Olesinski RW, Abbaschian GJ (1985) Bull Alloy Phase Diag 6:359
11. Merkwitz M (1997) Ph.D. Thesis, Chemnitz University of Technology
12. Merkwitz M, Weise J, Thriemer K, Hoyer W (1998) Z Metallkd 89:247
13. Kaban I, Hoyer W, Merkwitz M (2003) Z Metallkd 94:831
14. Hoyer W, Kaban I (2006) Rare Met 25:452
15. Kaban IG, Hoyer W (2008) Phys Rev B 77:125426
16. Iida T, Guthrie RIL (1993) The physical properties of liquid metals. Oxford University Press, New York
17. Hoyt JJ (1990) Acta Metall Mater 38:1405
18. Cahn JW, Hilliard JE (1958) J Chem Phys 28:258
19. Rowlinson SS, Widom B (1982) Molecular theory of capillarity. Clarendon Press, Oxford
20. Thompson DR, Rice OK (1964) J Am Chem Soc 86:3547
21. Schürmann HK, Parks RD (1971) Phys Rev Let 26:367